PAPER • OPEN ACCESS

Multi-view videogrammetry for the measurement of plate flexural vibration

View the article online for updates and enhancements.

Multi-view videogrammetry for the measurement of plate flexural vibration

R Rinaldo, P Gardonio, R Del Sal, L Dal Bo, E Turco, A Fusiello

DPIA, Università degli Studi di Udine, Via delle Scienze 206, 33100 Udine, Italy

E-mail: `roberto.rinaldo@uniud.it`

Abstract. This paper describes a simulation study of the measurement of the flexural deflection of a thin plate, excited by a transverse force at the fundamental frequency of the resonance modes, using an optical system consisting of multiple cameras. The estimate of the amplitude of the vibration is obtained starting from two or more sequences of images taken by the cameras, by means of triangulation. In this paper, we assume that the system is calibrated, and we focus on the error resulting from pixellisation. The simplified optical model is used to simulate how the accuracy of the measurements varies with respect to: the distance of the cameras from the structure; the opening angle between pairs of cameras; the resolution of the cameras and their number. The aim of the work is to evaluate the influence of the cameras arrangement on the measurement quality, and in particular if the use of a number greater than 2 cameras can allow a reduction of the measurement error, allowing a favorable compromise between spatial and temporal resolution of the cameras. As an example, the average error of the reconstruction of the first flexural deflection shape falls from 12% to 4%, when the measurement setup passes from 2 cameras to 12 cameras in the considered setup.

1. Introduction

The measurement of the vibrations of mechanical structures is of considerable interest in various fields of application, ranging from the design of surfaces (cars, trains, ships, etc) and air vehicles (helicopters, aircrafts, rockets). Optical techniques have received increasing attention in the literature, as, thanks to recent advances in optical hardware and computational power, they allow accurate vibration measurements without direct contact between the surface to be measured and the sensors. A complete review of the optical techniques used in the context of vibration measurements can be found in [1]. Among these techniques, this study focuses on image-based systems, which rely on photogrammetry and the reconstruction of scenes using digital images. In general, for the reconstruction of the 3D spatial configuration of the vibration, at least two views are required, which should be acquired with a high temporal speed and high spatial resolution. By means of triangulation, it is in fact possible to reconstruct the 3D transverse displacements produced by the vibrations of thin structures using point tracking (3DPT) [2, 3, 4] or digital image correlation (3DIC) [5, 6].

Some specific techniques proposed in the literature are based on single camera configurations. In [7], the authors propose a single camera stereo acquisition procedure using a four mirror adapter that creates artificial images with multiple views in the image sensor. These images are further processed to retrieve vibration information. A similar idea is considered in [8], where information on the periodicity of the vibration is exploited to limit the frame-rate of the camera.

Similar configurations are considered in [9, 10]. Although the idea of using multiple views and stereo acquisition systems has been presented in the literature, a quantitative analysis related to the use of multiple cameras, their arrangement and their characteristics is of paramount importance for the correct design of a measurement setup.

This paper presents a simulation study on a multi-view videogrammetry framework for the measurement of the flexural vibration field of a plate structure. In general, flexural vibrations of distributed structures cover rather large frequency bands, which for example can reach a few kHz for vibro-acoustic problems (see also [11]). Moreover, they present whole body deflection shapes, which depend on both the dynamic response of the structure, through their natural mode shapes and their modal density function, and on the spatial distribution and frequency content of the excitation field. Therefore, to measure flexural vibrations of distributed structures, high spatial-resolution and high frame-rate cameras should be employed. These are quite challenging requirements as the speed of the cameras depends both on their architecture (i.e. photosensor, ADC and data storage technologies) and on the amount of data ought to be processed in the time unit (i.e. requiring a trade-off between spatial and temporal resolution). The aim of this study is thus to investigate the advantages of multi-view videogrammetry for the measurement of flexural vibrations of distributed structures. To this end, a simulation study is presented, where the flexural deflection shape of a flat rectangular plate excited by a point harmonic force at its fundamental natural frequency is measured with multiple, i.e. more than two, cameras. Since the focus is on the multi-view arrangement, a 3D point tracking approach is considered, such that, as shown in sketch of Figure 1, the vibration field is reconstructed at a dense grid of marker points. Also, the study assumes the setup is perfectly calibrated such that the intrinsic (e.g. optic, etc.), and extrinsic (e.g. positioning, etc.) parameters of the cameras are known. In this way, the influence that the number of cameras and the cameras image pixelisation has on the accuracy of the measurement can be properly evaluated. The cameras are modelled with a classical pinhole model. The transverse vibration displacement of the plate is reconstructed from triangulation of the views recorded by the whole set of cameras, which are affected by errors due to pixelisation. The marker 3D position is computed by minimising the sum of the squared geometric distances between the measured and the projected image points in the cameras. In this way, it is possible to take advantage of the use of multiple cameras, determining 3D point positions by minimising the overall projection errors. Our work demonstrates that the use of multiple cameras actually improves the quality of the vibration estimate, even using cameras with limited spatial resolution. This allows a favorable balance with respect to the temporal resolution that may be required. Furthermore, the simulations presented allow to evaluate the influence of the arrangement and of the characteristics of the cameras in an experimental setup.

2. Plate vibration measurement

This section introduces the vibration model of a thin flat rectangular plate mounted on a rigid baffle. The mathematical formulation governing the flexural vibration of the structure is briefly recalled. It also describes the model and the mathematical formulation used to simulate the measurement with multiple cameras of the flexural vibrations of the plate. Since the aim of the study is to investigate the intrinsic properties of bending vibration measurement with image-based systems, a 3D-point tracking (3DPT) approach is employed [12, 13, 14] assuming perfect image detection of the target points.

2.1. Plate vibration model.

As shown in Figure 1, the flexural vibration and sound radiation of the plate as well as the locations of the cameras are defined with reference to the so-called world coordinate frame of reference $X, Y, Z,$, which is located at the centre of the plate. In the formulation, Cartesian x, y, z coordinates will be used to define the positions of the markers on the plate. Alternatively,
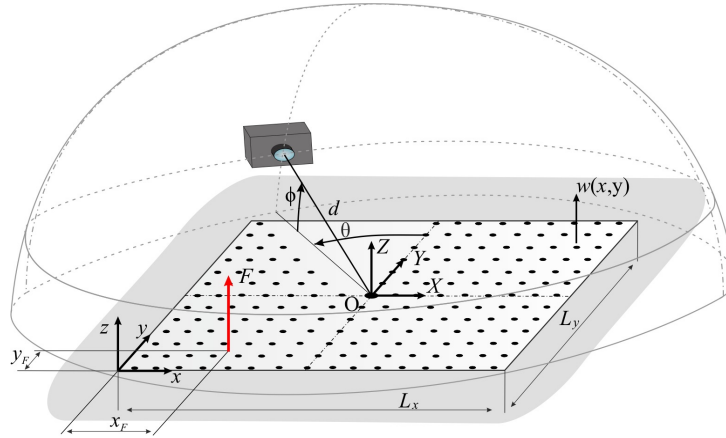
Figure 1. Model problem for the measurement of flexural vibration of a baffled simply supported plate.

polar r, θ, ϕ coordinates, referred to the world coordinate system, will be adopted to define the positions of the cameras, where r is the radius, θ is the azimuthal angle and ϕ is the elevation angle (see Figure 1). In this study, the cameras will be oriented in such a way as their optical axis points to the centre of the plate, that is, to the origin of the world system of reference. Also, the rectangular photosensitive sensor is tangent to an imaginary hemisphere centred in the middle of the plate and has lateral edges oriented parallel to the meridian and parallel arches of the hemisphere passing through the point of tangency.

Assuming classical plate theory [15], the time-harmonic flexural displacement of the plate at position x, y can be described by the following modal summation

$$w(x, y, t) = \text{Re}\{\sum_{n=1}^{\infty} \phi_n(x, y) \, q_n(\omega)\}. \tag{1}$$

In (1), $\phi_n(x, y)$ and $q_n(\omega)$ are respectively the shape functions and the complex flexural natural modes. For a simply supported plate, considering the Cartesian coordinates, the shape functions are given by [16]:

$$\phi_n(x, y) = 2 \sin\left(n_1 \frac{\pi x}{L_x}\right) \sin\left(n_2 \frac{\pi y}{L_y}\right), \tag{2}$$

where L_x, L_y are the surface dimensions of the plate, and $n_1 = 1, 2, \ldots$, and $n_2 = 1, 2, \ldots$, are the modal indices for the n-th mode. Also, the complex flexural modes are given by

$$q_n(\omega) = \frac{\phi_n(x_F, y_F)}{M[\omega_n^2 + j2\zeta\omega_n\omega - \omega^2]} F_0(\omega)e^{j\omega t},$$

where M is the plate mass, x_F, y_F are the coordinates of the excitation point force $F(x_F, y_F, t) = \text{Re}\{F_0(\omega)e^{j\omega t}\}$, and ω_n is the natural circular frequency [16]. In general, the response at each frequency will be controlled by the modes with natural frequencies close to the excitation frequency. In particular, when the plate is excited at the natural frequency of the first few natural modes, the response can be expressed in terms of the modal contribution of the resonant mode only. More specifically, for the excitation at the first few natural frequencies such that $\omega = \omega_n$, the displacement can be well approximated as

$$w(x, y, t) \simeq \phi_n(x, y) \, \text{Re}\{q_n(\omega)\}. \tag{3}$$

In our simulations, the transverse displacement $w(x, y, t) \simeq \phi_n(x, y) \operatorname{Re}\{q_n(\omega)\}$ of the plate marker at position x, y is calculated at the time instants when $w(x, y, t)$ is maximum. In a practical setting, knowing that $w(x, y, t)$ has a sinusoidal trend over time, its maximum amplitude can be calculated from samples obtained at regular time instants. Table 1 reports the characteristics of the simulated plate.

Table 1. Geometry and physical properties of the plate setup.

Parameter	Value
Lateral dimensions	$L_x = 668\,[\mathrm{mm}], L_y = 443\,[\mathrm{mm}]$
Thickness	$h = 19.8\,[\mathrm{mm}]$
Density	$\rho = 7200\,\left[\mathrm{kg/m^3}\right]$
Young's modulus	$E = 14 \times 10^{10}\,\left[\mathrm{N/m^2}\right]$
Poisson ratio	$\nu = 0.31\,[-]$
Modal damping ratio	$\zeta = 0.02\,[-]$
Position of the force	$x_F = 55\,[\mathrm{mm}]\,y_F = 23\,[\mathrm{mm}]$
Grid of markers	$N_x \times N_y = 15 \times 10$
Dimensions of the mesh elements	$d_x = 44.5\,[\mathrm{mm}], d_y = 44.3\,[\mathrm{mm}]$

2.2. Pinhole model and 3D point reconstruction.
Two or more cameras will be used to reconstruct the flexural vibrations of the plate using 3D Point Tracking. This study will assume the markers identifying the measurement points on the plate have infinitesimal dimension. Also, it will be assumed their projection onto the photo sensor of the cameras can be satisfactorily modelled with the classical pinhole camera model. The 2D position of the projection of a 3D point onto the camera plane can be modelled as

$$\mathbf{m} = \mathbf{PM}, \tag{4}$$

where $\mathbf{M} = [X, Y, Z, 1]^T$ is the homogeneous vector with the world coordinates of the point $\mathbf{M}$ and $\mathbf{m} = [u, v, 1]^T$, is the homogeneous vector with the image coordinates of the projections of $\mathbf{M}$ into the image plane of the camera. Also, matrix $\mathbf{P}$ is the camera projection matrix, which depends on its *intrinsic* and *extrinsic* parameters, specifying camera calibration and its position relative to the world coordinate system, respectively. In particular,

$$\mathbf{P} = \mathbf{K}\,[\mathbf{I}|\mathbf{0}]\,\mathbf{G},$$

where the intrinsic parameter matrix is given by

$$\mathbf{K} = \begin{bmatrix} \alpha_u & \alpha_u \gamma & u_0 \\ 0 & \alpha_v \hat{r} & v_0 \\ 0 & 0 & 1 \end{bmatrix}.$$

Here $\alpha_u = f k_u$ and $\alpha_v = f k_v$, and $1/k_u, 1/k_v$ are the width and height of the pixel footprint on the camera photosensor, and f is the camera focal length. Also, u_0, v_0 are the coordinates in pixel of the centre of the image plane. Finally, γ and $\hat{r}$ are the skew and aspect ratio parameters, which are normally given by $\gamma = 0$ and $\hat{r} = 1$ for most cameras [14], as it will be assumed in the simulations. The extrinsic parameter matrix is given by

$$\mathbf{G} = \begin{bmatrix} \mathbf{R} & \mathbf{t} \\ \mathbf{0} & 1 \end{bmatrix},$$

which is composed by the 3×3 rotation matrix $\mathbf{R}$, the 3×1 translation vector $\mathbf{t}$, specifying the rigid transformation between the camera and the world coordinate systems, and the 1×3 vector of zeros $\mathbf{0}$.

With $N \geq 2$ cameras, each projection provides one equation of the form (4), which can be cast in the system of equations

$$\mathbf{m}_i \times \mathbf{P}_i \mathbf{M} = \mathbf{0}, \; i = 1, ..., N. \tag{5}$$

From at least two of these equations, in principle, the 3D position of the point can be calculated. However, projection coordinates $\mathbf{m}_i$ are affected by errors. The errors can arise due to noise and other multiple factors, but the most important one is due to pixelisation, deriving from the spatial resolution of the image sensor. Due to the errors, equations (5) can not be satisfied exactly, and a least-squares solution is sought, With multiple cameras, the 3D position is estimated as a mean squared error minimisation considering all the projections, so we expect an improvement of the estimate. The Singular Value Decomposition (SVD) method can be used to this purpose [14], thus taking into account all the projections and minimising the overall estimation error for $\mathbf{M}$.

3. Parametric Study

The aim of this section is to investigate how multiple cameras can increase the accuracy of flexural vibration measurements of a plate structure. The formulation presented in Section 2 for the flexural response of a plate and for the optical measurement of displacements by means of triangulation are employed to simulate the measurement of the flexural response of the plate. The analysis considers the measurement of the first three flexural deflection shapes of the plate at the first three fundamental resonance frequencies. The reference deflection shapes are derived from Eq. 3. A comprehensive analysis is provided, which shows how the following parameters affect the measurement of the plate flexural response by means of triangulation with a pair or multiple of cameras, namely,

 (i) the radial distance d of a pair of cameras from the centre of the plate;

(ii) the aperture angle α between a pair of cameras;

(iii) the resolution of a pair of cameras;

(iv) the number of cameras in setups composed by more than 1 pair of cameras.

In the following, the accuracy of the vibration measurement is studied considering the following root mean square error over the $N_t = N_x \times N_y$ grid of plate marker points $P_i = (x_i, y_i)$

$$E_w = \frac{\sqrt{\frac{1}{N} \sum_{i=1}^{N_t} (w_i - \hat{w}_i)^2}}{w_{max}} 100 \quad (\% \text{ rel.to } w_{max}).$$

In this equation, $w_i = w(x_i, y_i, t), \hat{w}_i = \hat{w}(x_i, y_i, t)$ are respectively the actual and measured transverse displacements and $w_{max} = \max_{i=1,\cdots,N} \{|w(x_i, y_i, t)|\}$ is the maximum actual transverse displacement, at the time instants where the displacement is maximum. The simulation results are reported in a standard framework, which shows on the top a table with the values of the other parameters, kept fixed during the simulation, and then (a) a sketch of the measurement setup with highlighted the varied parameter; (b) a representation of the ideal flexural deflection shape; (c) the measured flexural deflection shape: for clarity, only the best and worst cases are shown; (d) the percentage average error with respect to the maximum displacement of the plate (colored lines).

Fig. 2 shows the accuracy of the reconstruction of the plate first flexural deflection shape with a pair of cameras arranged with fixed azimuthal θ and elevation ϕ angles and increasingly

	Radial distance d (mm)	Elevation angle ϕ (DEG)	Azimuth angle θ (DEG)	Aperture angle α (DEG)	Resolution (pixel)
Values	650 750 1000 1500	25	±30	60	320×180

(a)   (b)

(d)   (c)
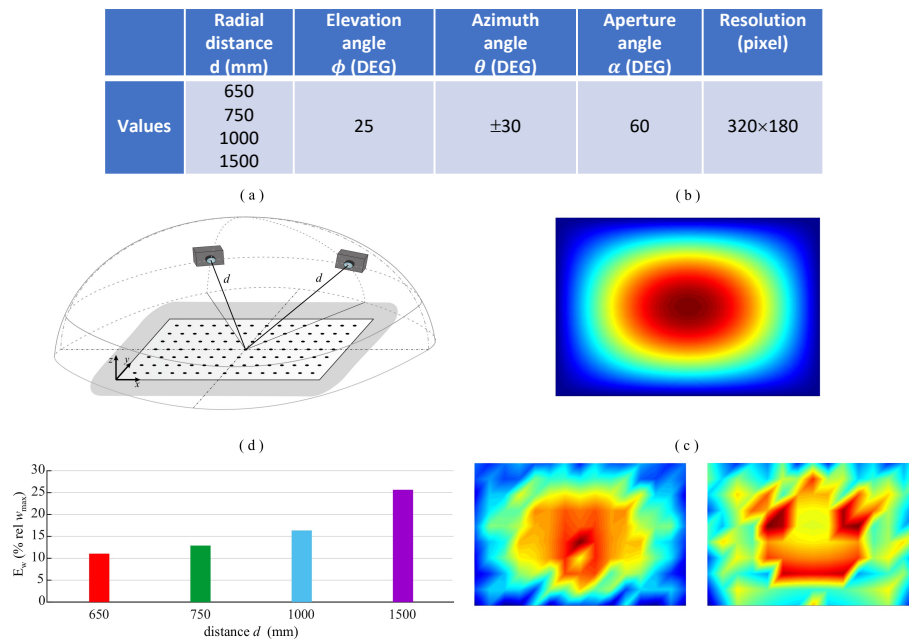

Figure 2. (a) distance case study; (b) ideal flexural deflection shape of the plate; (c) comparison between reconstructed flexural deflection shapes of the plate for the smallest (left) and largest (right) distances d; (d) bar graph of the mean error.

larger distance d. Note that the resolution of the two cameras is rather low (320×180 pixels). The results presented in Fig. 2 suggest that the accuracy of the measurement decreases as the distance of the cameras from the centre of the plate is increased. For example, according to the bar Plot (d) in Fig. 2, the average reconstruction error of the first deflection shape grows from about 12% to about 26% when the distance of the cameras is increased from 650 to 1500 mm.

Figures 3-4 show the results relative to the variation of the aperture angle between cameras, at different placements with respect to the plate. Figures 5 shows the estimation accuracy dependance with respect to the camera resolutions. More interestingly, Figures 6-7 show the estimation accuracy as a function of the number of low resolution cameras, with different placements with respect to the plate.

The results presented above provide an abstract of a comprehensive analysis, which considered a full range of camera configurations and additional vibration fields controlled by higher order flexural natural modes. All analyses confirmed the following conclusions with respect to the range of the considered parameters: 1) the distance of the cameras influences significantly the vibration measurement; 2) the angle of opening between a pair of cameras laid on a circle parallel to and centred on the plate, such that the cameras have a small elevation angle and variable azimuthal angle, does not influence much the vibration measurement; 3) alternatively, the angle of opening between a pair of cameras laid on a half-circle oriented on a vertical plane passing through the horizontal axis, such that the cameras have a variable elevation angle and fixed azimuthal angle, moderately influences the vibration measurement; 4) the spatial resolution of the cameras has a significant effect on the accuracy of the vibration measurement; 5) setups with more than 2 cameras significantly increase the accuracy of vibration measurements. For instance, Fig. 6, considering the reconstruction of the first flexural deflection shape, shows that, when the measurement setup passes from 2 cameras to 12 cameras the average error of the measurement falls from 12% to 4%.
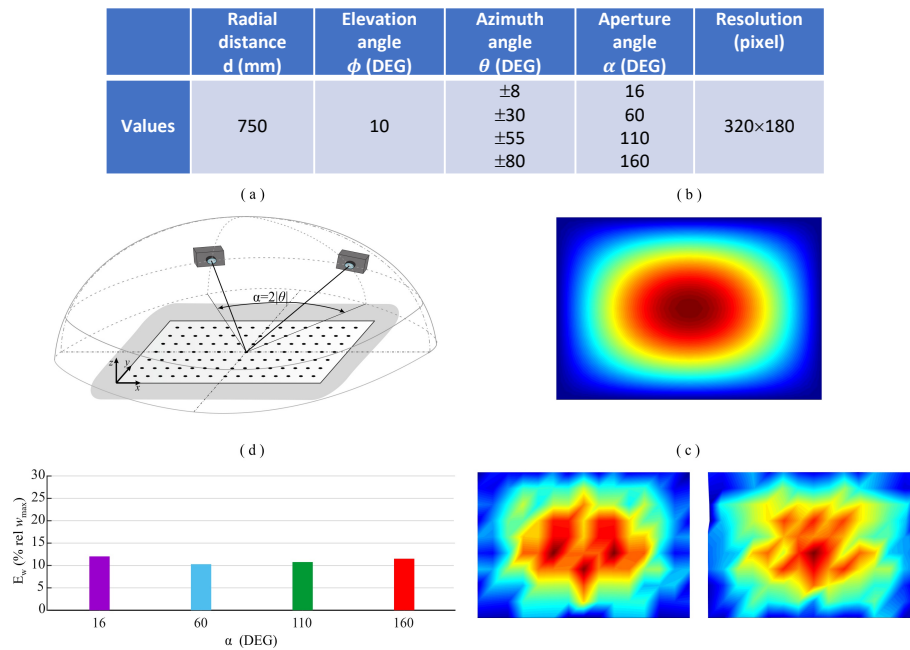
	Radial distance d (mm)	Elevation angle ϕ (DEG)	Azimuth angle θ (DEG)	Aperture angle α (DEG)	Resolution (pixel)
Values	750	10	±8 ±30 ±55 ±80	16 60 110 160	320×180

Figure 3. First deflection shape: (a) aperture angle case study ($\alpha = 2|\theta|$); (b) ideal flexural deflection shape of the plate; (c) comparison between reconstructed flexural deflection shapes of the plate for the smallest (left) and largest (right) azimuthal angle θ (d) bar graph of the mean error.

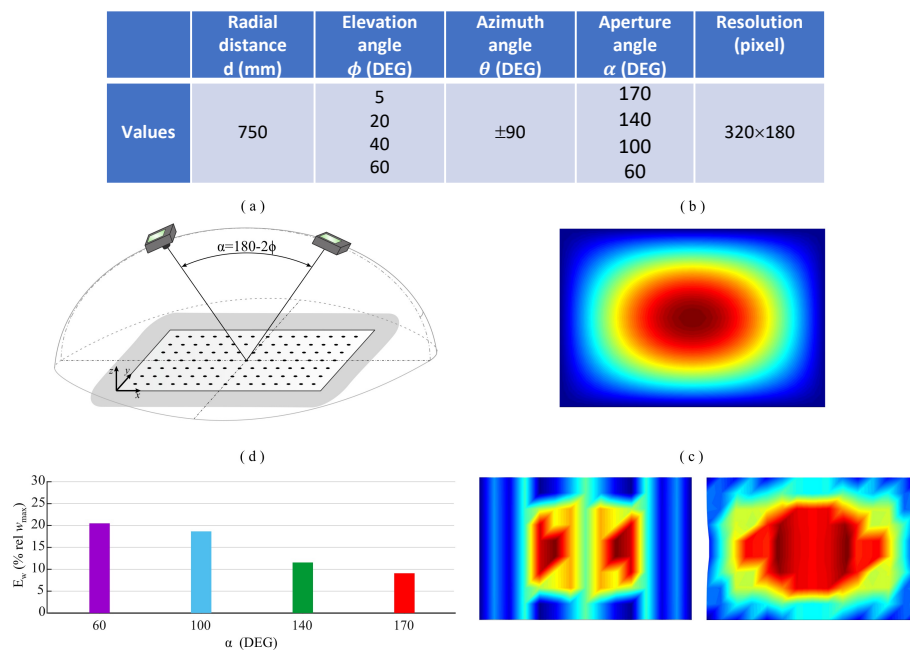|	Radial distance d (mm)	Elevation angle ϕ (DEG)	Azimuth angle θ (DEG)	Aperture angle α (DEG)	Resolution (pixel)
Values	750	5 20 40 60	±90	170 140 100 60	320×180

Figure 4. First deflection shape: (a) aperture angle case study ($\alpha = 180-2\phi$); (b) ideal flexural deflection shape of the plate; (c) comparison between reconstructed flexural deflection shapes of the plate for the largest (left) and smallest (right) elevation angle ϕ; (d) bar graph of the mean error.

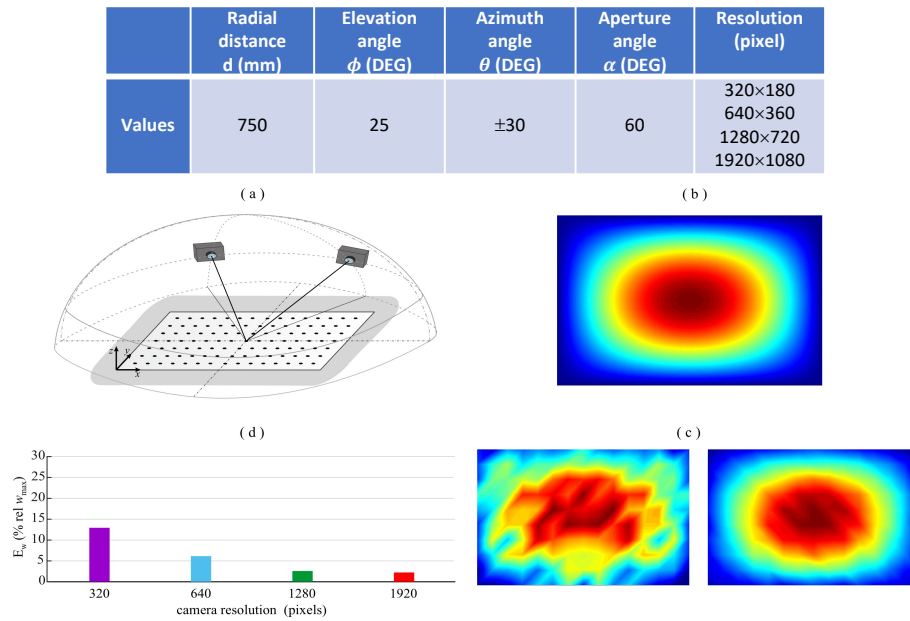|	Radial distance d (mm)	Elevation angle ϕ (DEG)	Azimuth angle θ (DEG)	Aperture angle α (DEG)	Resolution (pixel)
Values	750	25	±30	60	320×180 640×360 1280×720 1920×1080

Figure 5. First deflection shape: (a) resolution case study; (b) ideal flexural deflection shape of the plate; (c) comparison between reconstructed flexural deflection shapes of the plate for the smallest (left) and largest (right) resolution; (d) bar graph of the mean error.
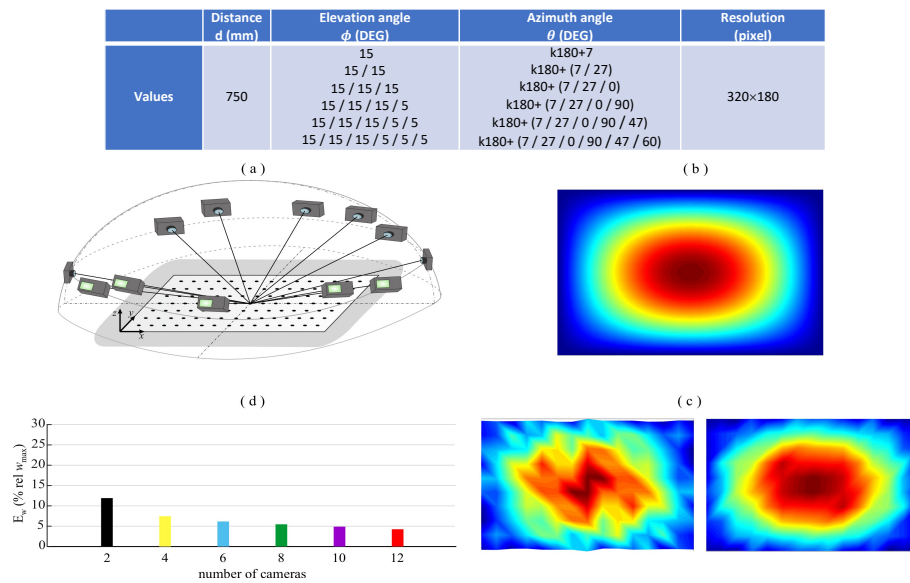

	Distance d (mm)	Elevation angle ϕ (DEG)	Azimuth angle θ (DEG)	Resolution (pixel)
Values	750	15 15 / 15 15 / 15 / 15 15 / 15 / 15 / 5 15 / 15 / 15 / 5 / 5 15 / 15 / 15 / 5 / 5 / 5	k180+7 k180+ (7 / 27) k180+ (7 / 27 / 0) k180+ (7 / 27 / 0 / 90) k180+ (7 / 27 / 0 / 90 / 47) k180+ (7 / 27 / 0 / 90 / 47 / 60)	320×180

Figure 6. First deflection shape: (a) multiple cameras case study; (b) ideal flexural deflection shape of the plate; (c) comparison between reconstructed flexural deflection shapes of the plate for the smallest (left) and largest (right) number of cameras; (d) bar graph of the mean error.
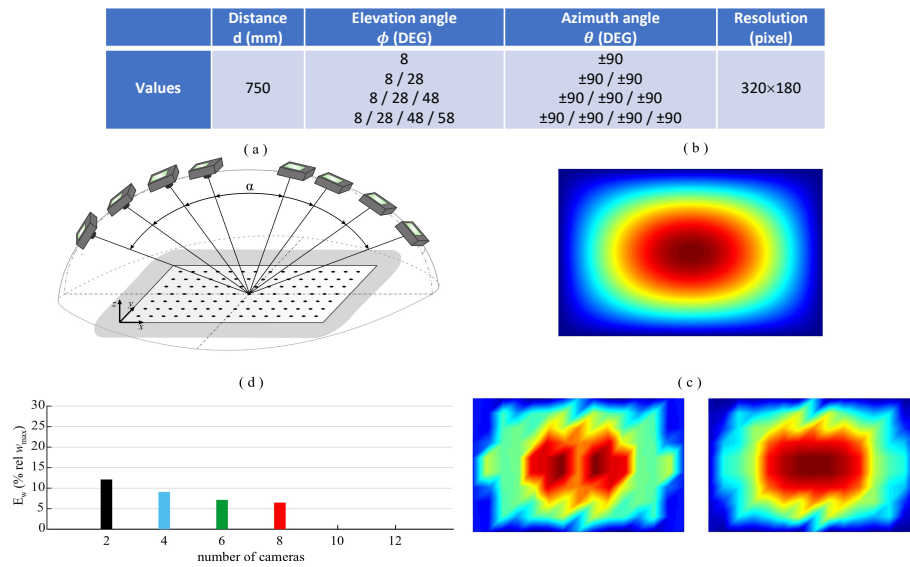
	Distance d (mm)	Elevation angle ϕ (DEG)	Azimuth angle θ (DEG)	Resolution (pixel)
Values	750	8 8 / 28 8 / 28 / 48 8 / 28 / 48 / 58	±90 ±90 / ±90 ±90 / ±90 / ±90 ±90 / ±90 / ±90 / ±90	320×180

Figure 7. First deflection shape: (a) multiple cameras case study; (b) ideal flexural deflection shape of the plate; (c) comparison between reconstructed flexural deflection shapes of the plate for the smallest (left) and largest (right) number of cameras; (d) bar graph of the mean error.
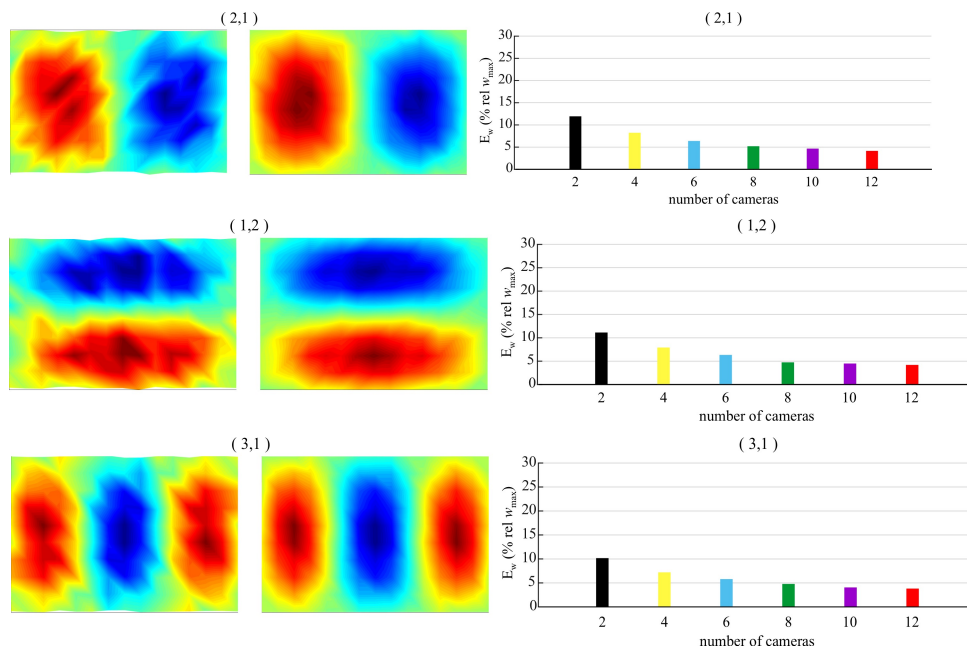

Figure 8. (a) multiple cameras case study; (b) comparison between reconstructed flexural deflection shapes of the plate for the smallest (left) and largest (right) number of cameras; (d) bar graph of the mean error.

9

4. Conclusions

In this paper, a comprehensive simulation study has been presented, in order to evaluate how the placement, resolution, and number of cameras affect the accuracy of the estimation of vibrations of mechanical structures. To this purpose, a simplified simulation arrangement has been considered, where errors are generated by pixelisation of images taken from the cameras. As case study, the vibration field generated by a plate structure has been considered, where 3D marker positions are reconstructed via triangulation. The principal objective was to assess if the use of multiple low-resolution cameras could improve the quality of the vibration estimate. As mentioned above, this allows a favorable balance with respect to the temporal resolution that may be required by applications involving high frequency modes. The results presented in the paper have shown that the accuracy of the measurement of the flexural deflection shapes of a plate increases as: (1) the cameras are arranged as close as possible to the plate; (2) the cameras are separated by large azimuthal angles; (3) the optical axis of the cameras impinges the structure with small elevation angles; (4) the cameras present high resolutions; (5) the number of cameras is increased. In conclusion, this study has demonstrated the effectiveness of the implementation of a setup with multiple, relatively low-cost low-resolution cameras for increasing the accuracy of the measurements of flexural vibrations of distributed structures.

References

[1] Baqersad J, Poozesh P, Niezrecki C and Avitabile P 2017 *Mech. Syst. Signal Pr.* **86** 17–34
[2] Frank Pai P, Feng D and Duan Y 2013 *54th AIAA/ASME/ASCE/AHS/ASC Structures, Structural Dynamics and Materials Conference* pp 891–895
[3] Baqersad J, Niezrecki C and Avitabile P 2015 *Mech. Syst. Signal Pr.* **62-63** 284–295
[4] Poozesh P, Baqersad J, Niezrecki C, Avitabile P, Harvey E and Yarala R 2017 *Mech. Syst. Signal Pr.* **86B** 98–115
[5] Chen F, Chen X, Xie X, Feng X and Yang L 2013 *Opt. Laser. Eng.* **51** 1044–1052
[6] Gorjup D, Slavic J and Boltezar M 2019 *Mech. Syst. Signal Pr.* **133 106287** 143–152
[7] Yu L and Pan B 2017 *Mech. Syst. Signal Pr.* **94** 374–383
[8] Barone S, Neri P, Paoli A and Razionale A 2019 *Mech. Syst. Signal Pr.* **123** 143–152
[9] Bhowmicka S and Nagarajaiaha S 2020 *Journal of Sound and Vibration* **489 115657**
[10] Gorjup D, Slavic J, Babnik A and Boltezar M 2021 *Mech. Syst. Signal Pr.* **152 107456**
[11] Gardonio P, Rinaldo R, Del Sal R, Dal Bo L, Turco E and Fusiello A 2021 *Proceedings of the 14th Intl Conference on Vibration Measurements by Laser and Noncontact Techniques*
[12] Faugeras O 1993 *Three-Dimensional Computer Vision: A Geometric Viewpoint* (The MIT Press, Cambridge, MA)
[13] Trucco E and Verri A 1998 *Introductory Techniques for 3-D Computer Vision* (Prentice-Hall)
[14] Hartley R and Zisserman A 2004 *Multiple View Geometry in Computer Vision* (Cambridge University Press)
[15] Reddy J N 2007 *Theory and Analysis of Elastic Plates and Shells* (CRC Press)
[16] Leissa A W 1969 *Vibration of Plates* (NASA Reference Publications, Washington)